IEEE Access
Multidisciplinary | Rapid Review | Open Access Journal

Received October 7, 2020, accepted October 19, 2020, date of publication October 22, 2020, date of current version November 2, 2020.

Digital Object Identifier 10.1109/ACCESS.2020.3033191

Paper Based Chipless RFID Leaf Wetness Detector for Plant Health Monitoring

SHUVASHIS DEY, (Member, IEEE), EMRAN MD. AMIN, (Member, IEEE), AND NEMAI CHANDRA KARMAKAR, (Senior Member, IEEE)
Department of Electrical and Computer Systems Engineering, Monash University, Clayton, VIC 3800, Australia

Corresponding author: Shuvashis Dey (shuvashis.dey@monash.edu)

This work was supported in part by the Australian Research Council Discovery Project under Grant DP110105606.

ABSTRACT This paper presents the design and analysis of a paper-based chipless RFID sensor for wetness content measurement in plant leaves. The sensor is designed using a passive microwave resonator to measure the ambient physical parameter. The resonator is designed with a rectangular loop inductively coupled with an interdigital capacitor. The experimental analysis of the designed sensor is illustrated here to prove its efficacy. The resonator provides adequate backscattered signal for wireless measurement in the microwave frequency band. When interrogated with a couple of UWB antennas and a VNA, it yields accurate leaf wetness response of the plant. The commercial competence of this sensing device is validated through its experimental analysis on three different types of leaf samples. This sensor is suitable for plant health monitoring in any small-scale gardening applications such as nurseries and greenhouses.

INDEX TERMS Backscattered signal, chipless RFID, Internet of Everything (IOE), interdigital capacitor, microwave, resonator, sensitivity, UWB, VNA, wetness.

I. INTRODUCTION

Wireless sensors are the backbone of the Internet of Everything (IoE). According to Cisco's definition, IoE provides an intelligent networked connection by combining people, process, data and things [1]. IoE augments seamless information capturing and interpretation for data from every point of transactions. In this regard, low cost fully printable wireless sensor will impact the vision of IoE enormously. In this paper, a fully printable chipless RFID leaf wetness sensor is presented that can have huge potential for the precision agriculture-one of the most significant segments of IoE [2]. RFID (Radio frequency Identification) is a technology that utilizes radio frequency waves to automatically identify or track an object. A tag with encoded information is attached to the object which is read and captured by a remotely placed RFID reader [3]. The development of chipless RFID technology provides an added dimension to the field of RF identification. This technology encodes data into the tags by using electromagnetic signature instead of embedding silicon chips which is the standard practice for the conventional chip-based RFID systems. This eventually reduces the cost and enables the design of printable RFID tags [4]. Hence, chipless RFID systems can be combined with sensor and sensing technologies to offer low cost, simplistic solutions to a varied range of IoE applications [5]. Such sensors have a great potential in retail and supply chain, asset tracking, healthcare, transportation, biotech, pharmaceuticals, waste management, Anti-theft system as well as precision agriculture [5], [6].

Leaf wetness indicates the presence of water on the surface of a crop canopy. It is mainly caused by the intercepted water during precipitation or fog, excessive irrigation and dew [7]. The leaf wetness level is a good indicator of the water status in the whole plant. Information about water availability in plants helps researchers to have a better understanding of the causes of drought [8]. It also helps farmers to control the irrigation process by figuring out if the crops need water and the required amount [9]. The leaf wetness is a significantly important parameter for photosynthetic performance analysis and hence it can provide critical information about the plant's health [8]. The presence of excessive water content on the leaf surface often results in the germination and sporulation of many fungal diseases that affect plants. A proper insight on the level and duration of leaf wetness enables the farmers to assess the appropriate time and areas for using preventive measures like fungicide application [10]. From the above review, we understand that the leaf wetness sensors facilitate a direct measurement of plant hydration which can effectively and potentially replace its indirect estimation via soil

The associate editor coordinating the review of this manuscript and approving it for publication was Wanchen Yang.

FIGURE 1. Photograph of two commercial leaf wetness sensors (a) Decagon leaf wetness sensor [12] and (b) Agrihouse leaf sensor [13].

moisture or air temperature sensors. Such efficient measurement prevents the damage of plants, helps the augmentation of crop growth and saves water resources [11], [12].

Fig. 1 shows two commercial leaf wetness sensors under test. The Decagon dielectric leaf wetness sensor mimics the moisture condition of a real leaf by closely approximating its thermal mass and radiation properties. Hence this sensor can determine the presence and duration of moisture on the leaves precisely. This enables researchers in both the ecological and agricultural sectors to have a better understanding of water flow mechanics, nutrient uptake and crop growth performance [12]. The price range of these commercial leaf sensors varies from around $140-$290 which makes them difficult to be used by the farmers [13].

The paper presents the design and analysis of a novel low-cost and paper-based chipless RFID sensor for wetness measurement in plant leaves. This noninvasive plant health monitoring device is designed using a passive microwave resonator. The hearth of the designed resonator comprises of a rectangular loop inductively coupled with an interdigital capacitor via two horizontal strips. This sensing device can provide information about the condition of a specific plant by measuring its leaf wetness level. The objective of this paper is to:

- Design and perform experimental analysis on a fully printable paper based chipless RFID sensor for plant wetness monitoring.
- Extend the experiment for various tree leaves to show the consistency in results for plant wetness monitoring
- Observe the impact of various shape, size and weighted tree leaves on sensing frequency band and calibration curves.

The paper is organized as follows: Section II presents the theoretical correlation of leaf microwave properties with wetness variation while section III illustrates the detailed design of the paper-based sensor. Section IV discusses the working principle and touches the base of sensor calibration whereas section V analyses the experimentally obtained results of the proposed sensor followed by the Conclusion in section VI.

II. CORRELATION OF WETNESS VARIATION WITH LEAF MICROWAVE PROPERTIES

The microwave properties of plant tissue such as leaves have a strong dependence on its wetness factor. The amount of

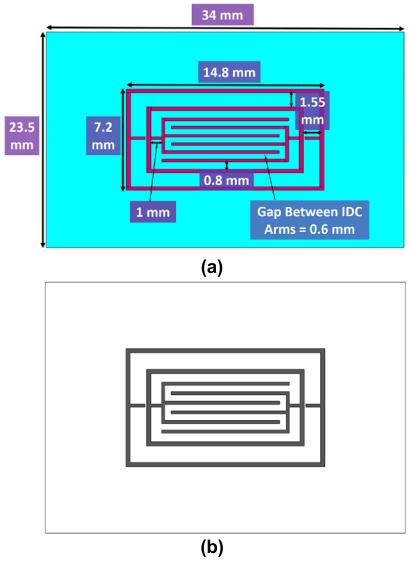

FIGURE 2. Proposed leaf wetness detector (a) CST Microwave Studio layout and (b) photograph of SATO printed paper-based tag.

stored water in a plant is an indicator of its health condition or freshness [8]. The dielectric permittivity of water at a given microwave frequency, f and temperature is specified by [14]–[16]:

$$\varepsilon_{fw} = \varepsilon'_{fw} + j\varepsilon''_{fw} \tag{1}$$

where the real and imaginary parts of free water permittivity ε_{fw} can be described using the Debye equation as follows [14]-[18] and [14]-[20]:

$$\varepsilon'_{fw} = \varepsilon_{w\infty} + \frac{\varepsilon_{w0} - \varepsilon_{w\infty}}{1 + (\omega\tau_w)^2} \tag{2}$$

$$\varepsilon''_{fw} = \frac{(\varepsilon_{w0} - \varepsilon_{w\infty})\omega\tau_w}{1 + (\omega\tau_w)^2} + \frac{\sigma_{eff}}{\omega\varepsilon_0} \tag{3}$$

Here, ε_0 is the permittivity of free space equal to 8.854×10^{-12} Fm^{-1}, ε_{w0} is the static dielectric constant of water and $\varepsilon_{w\infty} = 4.9$ is the high frequency limit of $\boldsymbol{\varepsilon}'_{fw}$, $\pi\omega = 2f$ is the angular frequency and τ_w is the relaxation time of water. The effective conductivity, σ_{eff} is the ionic conductivity due to dissolved salt or other ions in water [8], [14]–[20]. The given equations bestow the fact that both the real and imaginary parts of water dielectric permittivity are dependent on microwave frequency. As the plant leaves contain a certain water content, their dielectric properties are also a function of water dielectric permittivity at such frequencies. The dissipation factor or loss tangent is directly dependent on the ratio of real and imaginary dielectric constants. Therefore, variation in leaf water content will incur a change in the loss tangent. This alteration in loss tangent affects the signal transmission, a low dissipation factor reduces energy loss in the signal and therefore allows more power to be transmitted whereas it tends to block signal transmission with increasing loss tangent.

III. SENSOR DESIGN

Fig. 2 shows the proposed leaf wetness sensor with all its dimensions. The sensor is designed based on a horizontal

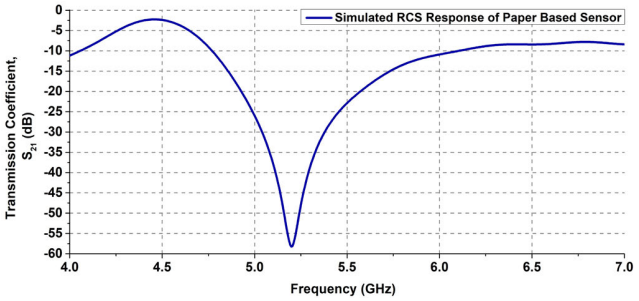

FIGURE 3. Simulated frequency response of designed leaf wetness detector.

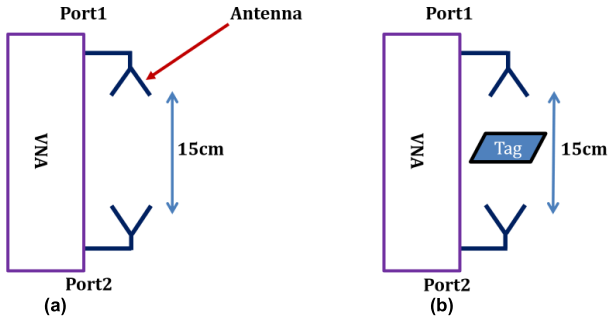

FIGURE 4. Interrogation system for chipless RFID based leaf wetness sensor (a) free space measurement (b) sensing-tag response measurement.

inter-digital capacitor (IDC) based resonator. Two rectangular loops are placed to surround the resonating arms of the IDC structure. These outer rectangular boxes are directly coupled to the IDC via two gap-coupled strips.

Such a combination of IDC structure coupled with the surrounding loops creates the resonating device. The outer boxes ensure the integrity of the entire resonator in the frequency spectrum. In other words, they prevent the signal interference of the IDC based resonator from the frequency response of any other surrounding element that can provide ID information (beyond the scope of this paper). Here, the IDC resonator is designed and optimized based on a systematic development from the ELC resonator. This resonator is chosen due to its planar and compact structure, low-cost and simplistic design as well as printability [21], [22]. IDC resonators can offer more sensitivity compared to their ELC counterparts by minimizing the electrical size and increasing the total capacitance [23]. In this case, by introducing the additional arms to ELC, the capacitance of the resonating structure is increased which in turn enhances the sensitivity. Due to the mirror symmetry of such structures, their resultant magnetic flux gets nullified which results in a pure electric resonance [23]. As a result, a strong electric field is created on the IDC resonator surface which easily gets perturbed by the presence and variation of a physical property such as leaf wetness [24]. This also causes the sensing resonator to provide high sensitivity and linearity. A comparative study of the IDC resonator with a number of conventional resonating structures also demonstrated its superior sensitivity over the others [25]. These are the very reasons why the IDC resonator-based sensor is selected for the leaf wetness sensing application. The sensor is designed on a low-cost paper substrate having dielectric constant, $\varepsilon_r = 2.31$ and loss tangent, $\tan\delta = 0.004$. The thickness of the paper substrate is 0.235 mm and the conductive silver ink for printing the resonant structure has a thickness of 450 nm. The conductivity of this ink is 6.2×10^5 S/m. The designed paper-based sensing device is printed by using the commercial SATO thermal printer and Fig. 2(b) shows its photograph [26]. Here, the paper substrate is chosen due to its high-water absorption ability. The simulated frequency response of the sensor is depicted in Fig. 3.

IV. WORKING PRINCIPLE AND SENSOR CALIBRATION

A typical chipless RFID system consists of a reader and a tag. The reader sends a wideband interrogation signal to the tag. The tags typically have the ID data incorporated and if enabled with a sensor, it can provide sensing information as well. Once interrogated, the tag sends a backscattered signal to the reader containing both ID and sensing related information. Along with backscattering, such data can be extracted via a retransmission-based technique as well. In this case, the reader incorporates a transmitting antenna which sends the interrogation signal to the tag and the acquired data from the tag is retransmitted further to a receiving antenna. Fig. 4 shows such an interrogation system of the proposed sensor. To simplify the analysis, this paper is only confined to the study of sensing aspect of the chipless RFID based sensing system and it does not incorporate any ID information. Here, the sensing mechanism incorporates a vector network analyzer (VNA) and a couple of co-polar Ultra-wide band (UWB) antennas which altogether function as a reader or interrogator. The printed paper-based sensing tag is attached to a leaf and placed in between the reader antennas which are used to interrogate the tag using RF pulse.

In order to obtain more clarity in the measured responses, a background subtraction technique is adopted in this case. This technique minimizes the effect of the environment in the measured sensor response [27], [28]. As observed in Fig. 4 (a), the transmission coefficient, S_{21} is measured as the initial reference or background (S_{21ref}) by leaving free space between the two UWB antennas. This essentially manifests to the measurement in the absence of a sensing tag and it involves the loading effect of the environment. Here, the environmental load may comprise of the reflection from surrounding objects, the antenna setup and the free space response of the interrogation system. Once the background response is obtained, the S_{21} response (S_{21tag}) of the sensing tag is measured by keeping the tag between the antennas as shown in Fig. 4 (b). Along with the frequency response of the tag, this signal also includes environmental loading. Hence, the calibrated transmission coefficient (S_{21cal}) can be calculated by subtracting the background response from that of the tag as shown in (4) [27], [28]. This S_{21cal} is used for all the measured results depicted throughout the paper [27], [28].

$$S_{21cal} = S_{21tag} - S_{21ref} \tag{4}$$

The wetness variation in leaves alters the electrical properties of the paper-based resonators which results in a deviation

FIGURE 5. Different plant types (a) Camellia flower (b) Blueberry (c) passionfruit.

in the frequency response of the sensing tag. In this regard, it is mention-worthy that the size, shape, weight, dielectric constant and other contributing factors that help to determine the condition of a leaf are quite diverse for different types of plants. The designed leaf wetness detector is dependent on the dielectric constant and quality factor of the leaf for its operation. Therefore, for monitoring a specific type of plant leaves, the sensor needs to be a calibrated on a case by case basis, rather than using a generalized detection scheme.

The calibration curve of a plant leaf sample is used as a reference to measure the wetness content of a random leaf from the specified plant. These curves can be extracted from the experimentally obtained results based on their respective sensing or operating frequency band. Depending upon the shape, size and weight, the sensing band of leaves of a specific plant can be different as well. This in turn necessitates the case by case calibration for different plant leaves. The techniques for forming a calibration curve is illustrated in the results section depicted below.

V. RESULTS

In the depicted analysis, leaves from three different plant types are used to illustrate the sensing capability of the designed leaf wetness detector. In this case, leaves from a flower plant namely camellia and two fruit plants namely blueberry and passionfruit are selected due to their different size, morphology and diversity as shown in Fig. 5. For each of the plant types, three different leaf samples are investigated to observe if they provide any consistent distinctive response for different wetness levels.

Fig. 6 shows the measured reflection coefficient of one of the UWB antennas used in the leaf wetness measurement experiment. It can be seen that the antenna occupies a UWB

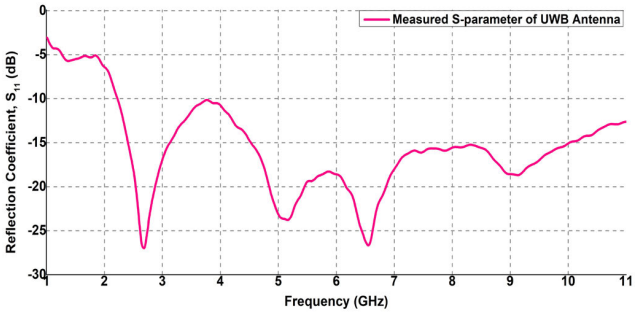

FIGURE 6. Measured frequency response of the UWB reader antenna.

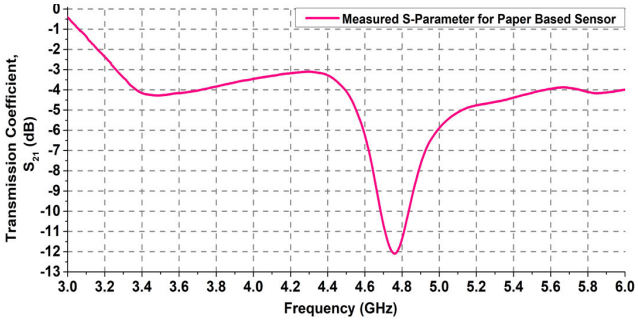

FIGURE 7. Measured frequency response of printed leaf wetness detector.

band of 2.2-11 GHz with a return loss greater than 10 dB for the entire bandwidth. It is noteworthy that both the reader antennas used in this analysis are identical and hence they have a similar frequency response.

A. S-PARAMETER MEASUREMENT

Fig. 7 depicts the measured transmission coefficient of the printed paper-based leaf wetness detector in free space. It can be observed that the sensor exhibits a resonance notch at around 4.8 GHz with an amplitude depth of about 8 dB. This indicates that though the paper-based sensor is designed with low precision and with a very thin conducting track, the backscattering signal is significantly high enough for wireless detection. The measured response shows a resonance shift of the resonator towards a lower frequency in comparison to its simulated version depicted in Fig. 3. This occurs due to the printing resolution of the SATO printer along with the deviation of paper and conductive ink properties from the ideal case used in the simulation.

B. EXPERIMENTAL ANALYSIS ON DESIGNED LEAF WETNESS DETECTOR

After the successful frequency response measurement of the sensor, it is applied to the leaf of a plant and measured with the Agilent VNA and two UWB reader antennas. Fig. 8 shows the photograph of the measurement set up. When overlaid on a leaf, the frequency response of the sensor encounters a deviation from its free space counterpart depicted in Fig. 7. These responses vary according to the characteristics of the specified leaves. The leaf under test is placed in between the reader antennas and data are extracted as their transmission coefficients.

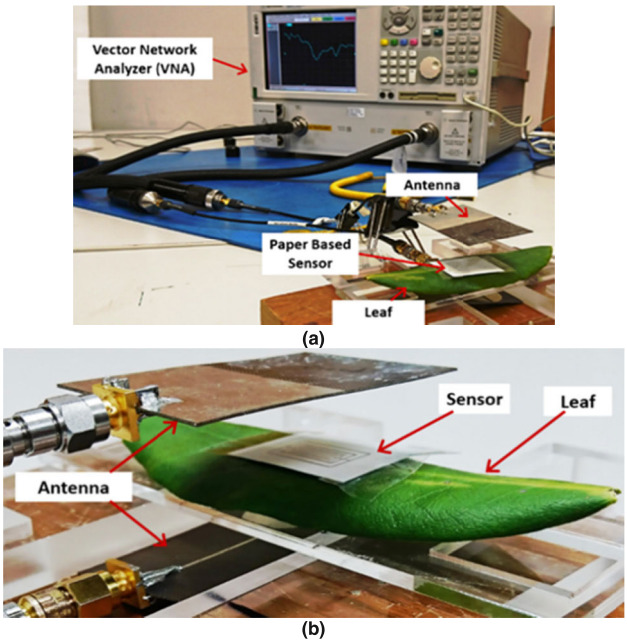

FIGURE 8. Experimental set up of the leaf sensor (a) with VNA and antennas and (b) close-up view.

The wetness content of the leaf is varied by drying it up with a certain controlled temperature using an oven. In this case, the frequency response extraction starts with a fresh leaf, which is considered to have 100% (w/w) water contents. As the leaf is dried up, its weight percentage starts to get reduced. The reduced weight percentage is calculated using (5), as given below.

$$X = \left(\frac{P}{100}\right) * W \tag{5}$$

where X = reduced weight for drier samples in grams (compared to the initial weight), P = weight percentage of leaf and W = initial weight for fresh samples in grams (at P = 100%). During the experiment for each of the wetness stages (starting from fresh to completely dry), the weight of the leaf is measured with a high precision low weight measuring scale. In order to maintain consistency in the wetness reduction, the weight percentages of all the leaves under test are decreased by a step of 10% from their respective initial values. It is observed that the leaves generally attain their dryness saturation at 60% weightage. Further exposure to temperature increment causes the leaves to become fragmented and therefore, they start to produce ambiguous responses.

Fig. 9 shows the comparative frequency responses of the sensor when it is overlaid on various fresh (100% weight percentage) leaf samples along with the sensor only response (in absence of leaf). Here, it is noteworthy that the Fig. 9 shows the sensing response of only one sample (Leaf-3) from each of the leaf type under consideration, namely, blueberry, camellia and passionfruit. As seen earlier in Fig. 7, when the sensor is not exposed to leaves, it resonates at around 4.8 GHz. The presence of leaves distorts the resonating

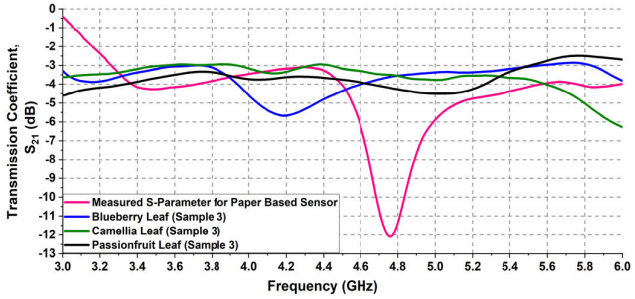

FIGURE 9. Comparative frequency response of proposed sensor for different leaf types.

waveform of the sensor completely. Based on their respective dielectric losses, different leaves impact the sensor in different manners.

For example, when the sensor is overlaid on blueberry sample leaf −3, the resonating waveform shifts to a low-frequency value of around 4.2 GHz while a significant resonance amplitude reduction becomes evident. However, the sensor still exhibits a distinguishable resonance. From the analysis, it is found that all the blueberry leaf samples indeed show identifiable resonances. Nevertheless, the corresponding frequencies of these resonances vary from sample to sample which eventually does not allow a consistent resonance shift (due to wetness variation) across all the samples. In addition, for camellia and passionfruit leaves, the sensing resonance becomes almost indistinguishable which is evident from Fig. 9. In these cases, the sensing signal incurs an extreme amplitude reduction due to the very high dissipation factor or dielectric loss tangent of the leaves. The presence of water in leaf samples induces such high loss factor which eventually reduces the quality factor of the sensing signal. Given the random nature of biomaterials such as leaf, it is important to use a sensing mechanism which is consistent across the samples of an individual leaf type. The depicted leaf samples in this analysis either do not provide a consistent resonance shift across all the samples or they have no identifiable resonance. Therefore, instead of using resonance shift, the experimental analysis exploited the variation of sensing signal amplitude for detecting the difference between various wetness contents of a leaf sample.

1) CAMELLIA LEAF

The wetness measurement analysis of the sensor starts with camellia leaves. Fig. 8 specifically shows the wetness measurement setup for this type of leaves. As mentioned earlier, the study involves three different leaf samples whose wetness contents are lessened by exposing them in controlled temperature increment. As water level reduces, the weight of the leaves (turgidity) decreases. Table 1 depicts the weight percentage variation of the camellia leaf samples used in the experiment. For fresh samples, the weight percentage is 100% with their corresponding weight in grams. It is evident that for each of the samples, a reduction in weight occurs as they get drier. The values depicted in Table 1 are calculated by using (5).

TABLE 1. Weight variation of camellia leaves with change in wetness.

Weight Percentage, P (%)	Weight of Leaf-1 (g)	Weight of Leaf -2 (g)	Weight of Leaf -3 (g)
100	1.07	0.96	1.06
90	0.963	0.864	0.954
80	0.856	0.768	0.848
70	0.75	0.672	0.742
60	0.642	0.576	0.636

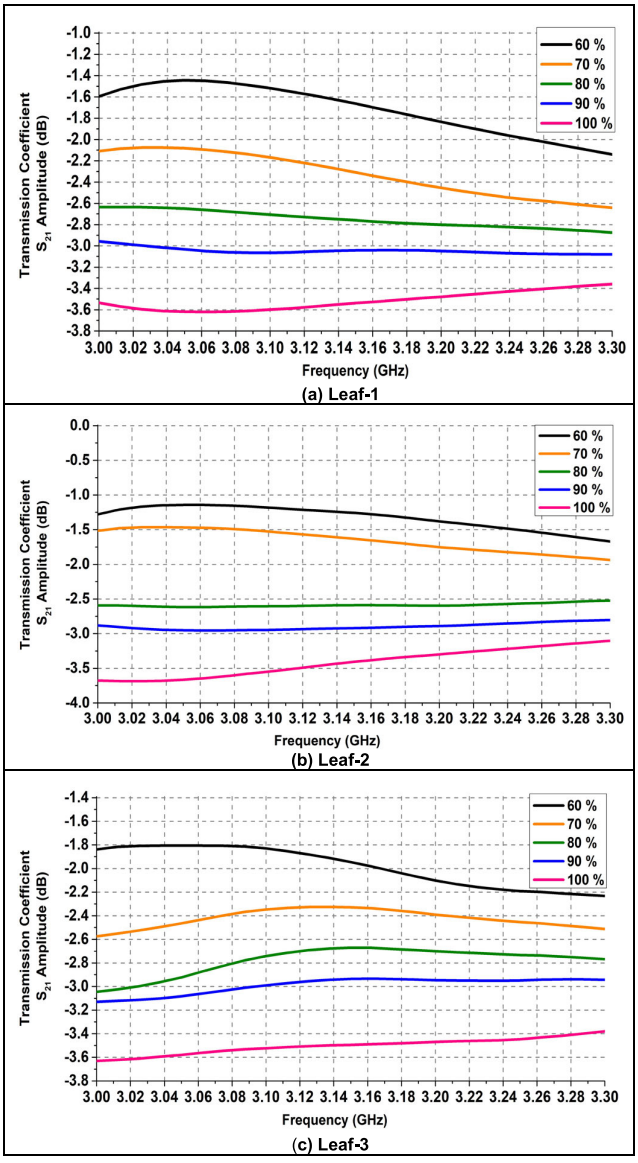

FIGURE 10. Frequency response of designed sensor for wetness variation in camellia leaves.

Fig. 10 shows the transmission coefficients of the leaf wetness detector for each of the camellia leaf samples at different wetness levels. It can be observed that for all the leaves, the signal corresponding to the fresh weight percentage (highest wetness level) has the lowest amplitude level. As the leaves are dried up, their weight percentages keep getting reduced and the resulting signal amplitude levels are increased. Eventually the signal corresponding to the completely dry condition exhibits the highest amplitude level

FIGURE 11. Blueberry leaf.

TABLE 2. Weight variation of blueberry leaves with change in wetness.

Weight Percentage, P (%)	Weight of Leaf-1 (g)	Weight of Leaf -2 (g)	Weight of Leaf -3 (g)
100	1.26	0.93	0.65
90	1.134	0.837	0.585
80	1.008	0.744	0.52
70	0.882	0.651	0.455
60	0.756	0.558	0.39

in the specified frequency zone. The reason for such consistency in the amplitude variation lies in the fact that the wetness reduction causes the signal transmission to get better. As the leaves become drier, their transmitted power level increases. Water has a high dissipation factor (0.157 at 3GHz) at microwave frequencies [29]. Therefore, higher wetness contents instigate an increased energy loss in the signal which forces to have a reduced transmitted power. Drying up the leaves decreases the water content which eventually helps to raise the power level.

It can be seen that each of the camellia leaf has the same sensing frequency zone from 3-3.3 GHz. The transmitted power for each leaf wetness content exhibits a distinct amplitude level in the entire specified frequency band. This distinction in amplitude allows the sensor to extract the wetness level of the leaf.

2) BLUEBERRY LEAF

The blueberry leaf samples used for wetness analysis significantly differ from each other in terms of weight. Fig. 11 shows a sample image of the blueberry leaf. The weight of different leaf samples at various wetness conditions are depicted in Table 2. It can be seen that the initial weight of the samples (at fresh condition) represent a gap of at least 0.28 grams. The measurement process of these leaf samples is the same as that of the technique depicted in the case of camellia leaf (Fig. 8). Here, the sensor overlayed samples are interrogated by two UWB antennas from a distance of 7.5 cm. It can be observed that the blueberry samples exhibit a similar response to that of the camellia as well. Fig. 12 shows the transmitted power amplitude variation of the specified blueberry leaf samples at different wetness levels. Here, all the samples have a sensing frequency zone of 3-3.3 GHz at which the transmitted power exhibits a distinct amplitude level for each of the corresponding leaf wetness content or weight percentage.

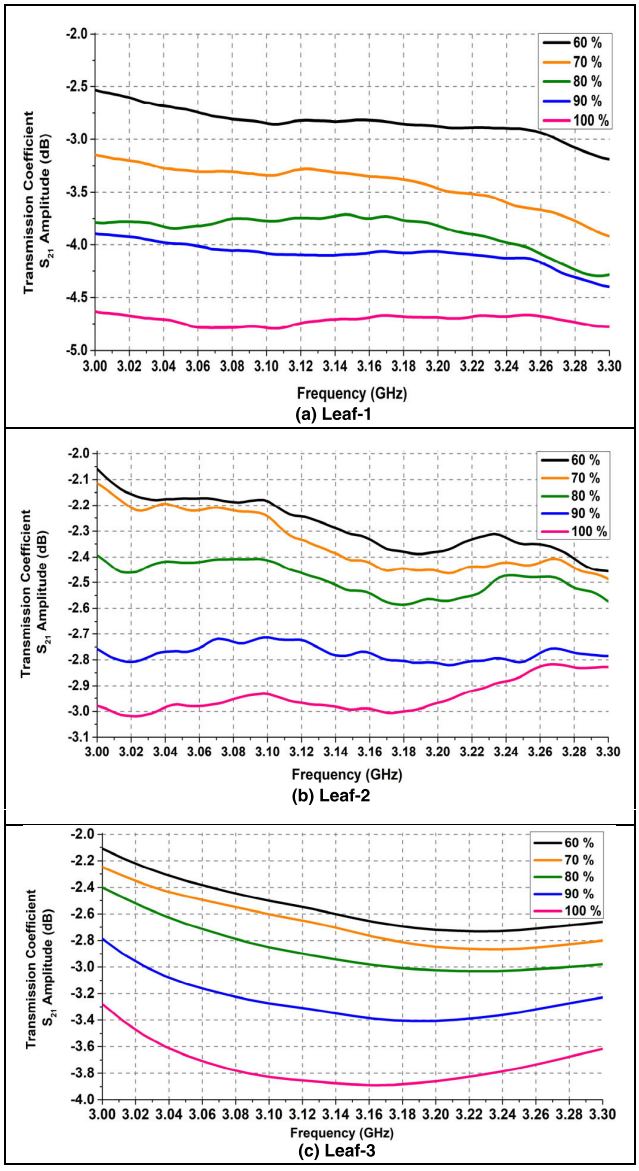

FIGURE 12. Frequency response of designed sensor for wetness variation in blueberry leaves.

As depicted in the case of camellia leaf samples, the transmitted power level for blueberry also increases with decreased leaf wetness contents. Reduction in the amount of stored water reduces the signal energy loss for these leaf samples as well.

3) PASSIONFRUIT LEAF

Fig. 13 shows the sample image of the passionfruit leaves used in the experiment. This type of leaves has a wide variety in their shape, size and weight. Some of them consist of three different lobes while others have only one. The juvenile leaves are quite light in weight when adult ones are comparatively thick and heavier.

Table 3 represents the weight variation of passionfruit leaf samples used in the wetness measurement experiment. Here, leaf 1 and 2 are adult leaves having one and three lobes respectively whereas leaf 3 is a small-sized juvenile leaf with

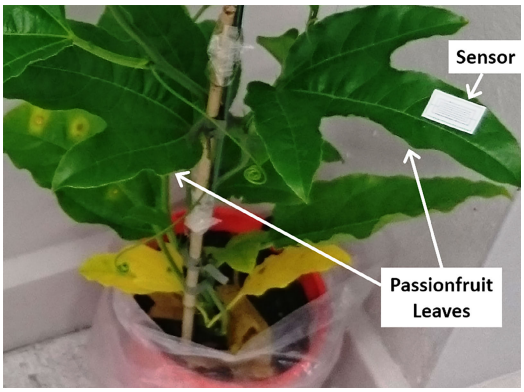

FIGURE 13. Passionfruit leaves.

TABLE 3. Weight variation of passionfruit leaves with change in wetness.

Weight Percentage (%)	Weight of Leaf-1 (g)	Weight of Leaf -2 (g)	Weight of Leaf -3 (g)
100	1.78	1.87	0.53
90	1.602	1.683	0.477
80	1.424	1.496	0.424
70	1.246	1.309	0.371
60	1.068	1.122	0.318

three lobes. When the leaf wetness detector is overlaid on these leaves, the obtained responses exhibit a similar characteristic in terms of signal amplitude. As shown in Fig. 14, for each of these leaves, the transmitted power amplitude level increases with weight percentage reduction. The weight reduction indicates a drop in the amount of stored water in leaves. Hence it can be said that the signal transmission gets better with leaf wetness reduction. This sensing feature is absolutely similar to the cases of other leaves used in the wetness measurement experiment. As observed in the earlier sections, the signal transmission power level improves with wetness reduction in camellia and blueberry leaves as well.

In the case of passionfruit leaves, however, the sensing frequency zones are not the same for all the leaves under consideration. Variation in shape and size of the leaf samples imposes a change in their dielectric permittivity values which in turn changes the sensitive frequency band of the respective samples.

Fig. 14 shows that for the single lobe adult leaf, the sensing zone is found at 3.6-4 GHz whereas the adult leaf with three lobes is sensitive at 4.26-4.46 GHz band. The juvenile leaf with three lobes exhibits its sensing zone at a higher frequency band starting from 4.6-5 GHz.

VI. SENSITIVITY ANALYSIS AND SENSOR DEPLOYMENT

Based on the experimental results depicted above, this section illustrates the sensitivity analysis of the sensor for different leaf types. It also discusses the deployment strategy of the sensor in a real-life environment along with the practical implementation challenges.

A. SENSITIVITY OF DIFFERENT LEAF SAMPLES

Fig. 15 shows the sensitivity or calibration curve for camellia leaves at 3.15 GHz. This frequency is chosen as it is the center frequency of the sensing zone although one could

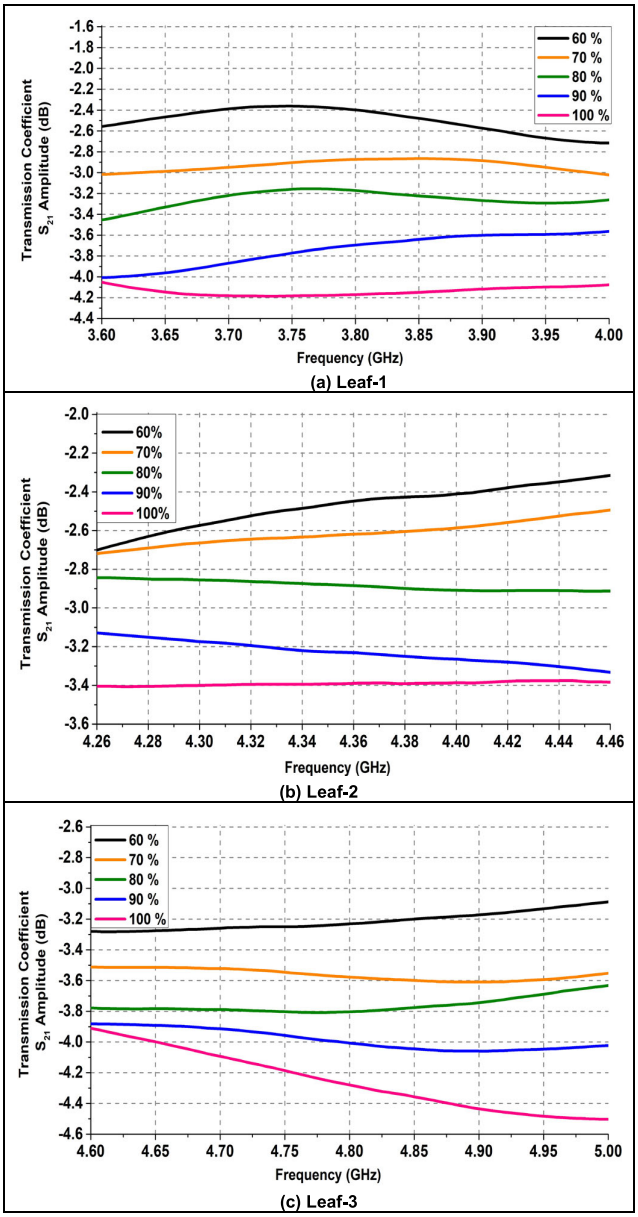

FIGURE 14. Frequency response of designed sensor for wetness variation in Passionfruit leaves.

choose any point in the specified frequency band for forming a calibration curve. To form the curve, the average of amplitude levels for all the leaf samples at a certain weight percentage is calculated. The camellia leaf samples do not vary much in terms of size, shape and initial weight; therefore, the amplitude levels of different leaf samples corresponding to a single weight percentage remain quite close to each other. At fresh condition, these values almost overlap while a bit of amplitude scattering is observed as the samples get drier. The depicted calibration curve (extracted from average values) exhibits an amplitude level gap of at least 0.25 dB (approximately) in between different leaf wetness contents. This curve can be used to detect the wetness level of any camellia plant. If the transmitted power amplitude level of the sensor is obtained for a random camellia leaf, it can be compared against the calibration curve which would provide

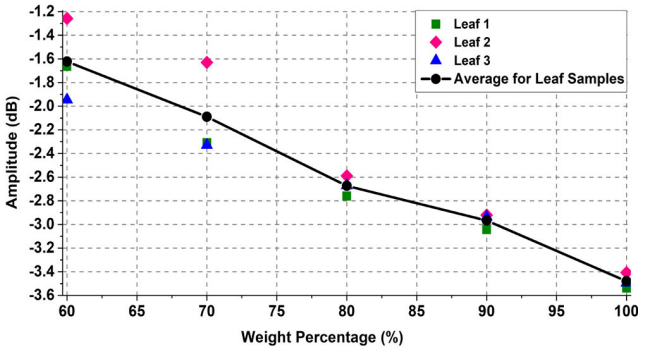

FIGURE 15. Sensitivity curve for different camellia leaf samples at centre of sensing frequency zone.

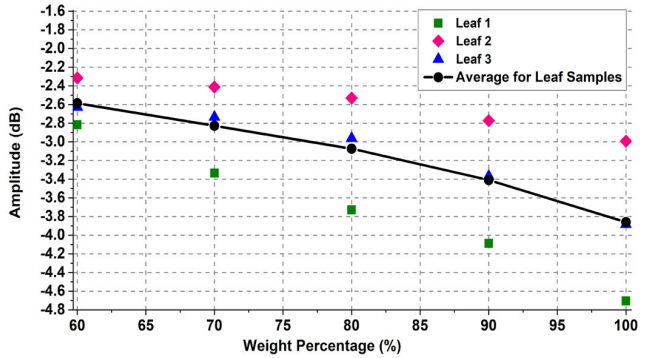

FIGURE 16. Sensitivity curve for different blueberry leaf samples at center of sensing frequency zone.

the corresponding weight percentage (turgidity) to indicate the freshness (wetness) level of the leaf.

Fig. 16 portrays the sensitivity or calibration curve for blueberry leaf, extracted from the average amplitude of three given samples. The power amplitude levels of the samples for a certain weight percentage illustrate an opposite trend compared to that of the camellia leaves. In this case, the amplitude levels of different samples are more scattered in fresh conditions which tend to become converged as the leaves are dried up. This phenomenon completely contrasts to that of camellia leaves where the power amplitude of samples starts to diverge with wetness reduction. Since the averaged calibration curve has a minimum amplitude level gap of about 0.3 dB, it can be used to detect the wetness level of an unknown blueberry leaf sample. However, as it is seen from Table 3, the blueberry leaves have a diverse weight range in general. Hence, for more precise detection of wetness level, the weight of the unknown sample can be measured beforehand to calibrate it against the reference leaf (used in the experiment) with similar weight percentage.

As mentioned earlier, the passionfruit leaves have different sensing zones based on their morphology. Fig. 17 shows the sensitivity curves of these leaf samples at the center of their respective sensing frequency band. A closer look at the curves depicts a minimum amplitude level gap of 0.2 dB in between different weight percentages. Hence, these curves can be used to obtain the wetness level of a passionfruit leaf. When wirelessly interrogated, the overlaid sensor on this leaf

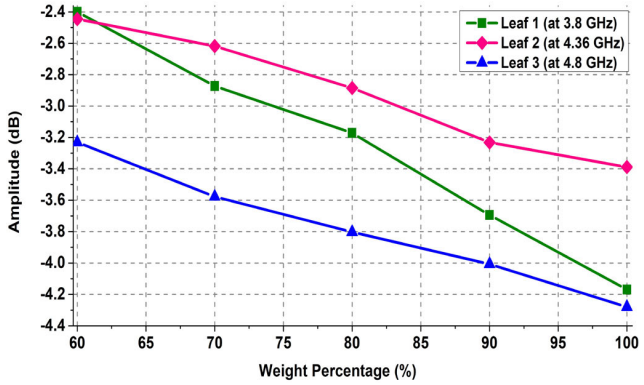

FIGURE 17. Sensitivity curves for different passionfruit leaves at center of their respective sensing frequency zone.

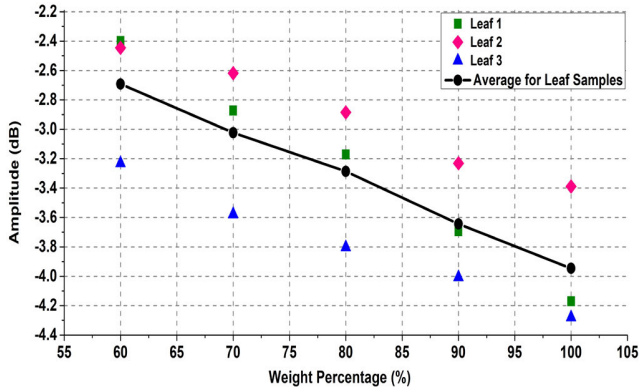

FIGURE 18. Average sensitivity curve for passionfruit leaves.

under test provides a certain amplitude level. This amplitude is compared with one of the calibration/sensitivity curves to find the corresponding weight percentage (turgidity) or wetness level. The required calibration curve against which this comparison is made can be determined based on the leaf's visual shape, age and number of lobes. If a precise shape, size, lobe number and age is not a concern and the user is only interested in any random passionfruit leaf, a rough wetness estimation irrespective of sensing frequency can be obtained from the average sensitivity curve depicted in Fig. 18.

B. PRACTICAL IMPLEMENTATION CHALLENGES AND DEPLOYMENT STRATEGY

The calibration curves portrayed in this paper have a significant role in determining the leaf wetness content from the measured amplitude levels. However, it can be seen that specificity poses a substantial challenge in this regard. Here, a particular amplitude level may often correspond with more than one specific weight percentages belonging to separate calibration curves. For example, a comparative look at the sensitivity curves of camellia (Fig. 15) and blueberry (Fig. 16) leaves shows that the same amplitude level of −2.7 dB indicates two separate weight percentages of 80% and 65% respectively. The dispersion of values depicted in the calibration or sensitivity curve plots also signifies that the amplitude level measurement does not provide a one-stop solution in determining the leaf wetness content. As the depicted sensitivity curves are specific to individual leaf types and morphology, having prior information on the weight, age and number of lobes of the particular leaf can be used to deal with the specificity and dispersion issues. Provided that the required information is known, the proposed sensing resonator can be overlaid on the leaf sample to extract its wetness content by using the calibration curves. As mentioned earlier, the measured amplitude level of the leaf sample would correspond to a weight percentage in the curve, which would eventually provide the specific leaf wetness content.

In this case, it is worthwhile to mention that the designed sensor is not a general-purpose leaf wetness detector. In order to detect the wetness variation in a particular plant, the sensor needs to be calibrated beforehand so that it can provide a standardized reference for the specific plant type. The requirement of such plant-specific standardization somewhat limits the application areas of this sensor. It cannot provide wetness information on a random plant in a field without prior calibration. Small gardens, nurseries or greenhouses generally deal with a limited number of trees or plant types. Therefore, they allow a calibration of the sensor for each type of plants present in the specified area and as a result, the leaf wetness level for these plants can be determined on a regular basis.

For practical implementation of this sensing system, multiple sensor nodes need to be deployed in the specific field under consideration. The experimental setup shown in this study is essentially used to provide a proof of concept of the system. However, for real-world deployment, a more sophisticated yet low-cost reader-based measurement would be required. Such reader modules incorporate both the transmitting and receiving antennas in their architecture [30], [31]. There has been an ongoing effort to develop low-cost, lightweight and portable readers in the chipless RFID research community. Sparkfun Electronics has recently introduced an inexpensive portable commercial reader named 'Walabot developer' that can be used to cover the ultra-wide band (UWB) frequency range [32]. Such a reader can be attached to a drone which may fly to a suitable location near the plants to interrogate the leaf sensor nodes. This can also resolve the short reading range issue of chipless technology. Using drone-mounted readers may incur additional cost to the interrogation system and therefore, it might not be the best affordable choice in many developing countries. In this case, leveraging the existing resources would be the most effective and realistic solution. The reader can essentially be mounted on such resources like center pivot booms, sprinklers or sprayers that regularly pass over the field. It can then extract the sensing information by scanning the leaf wetness detector.

VII. CONCLUSION AND FUTURE WORKS

In this paper, we have presented the design and analysis of a fully printable leaf wetness measuring sensor. The above analysis exemplifies the effectiveness of the microwave frequency design of an extremely low-cost paper-based leaf wetness detecting sensor. The designed sensor is simply

overlaid on different leaf samples to extract the data of their wetness contents. The experimental analysis utilises leaves from three different plant types, namely- camellia, blueberry and passionfruit. The sensor response for each of the leaf types demonstrates a common characteristic where the transmitted power amplitude level gets increased with reduced leaf wetness contents. This indicates an improvement in signal transmission as the leaf samples get drier. Each leaf sample provides a distinctive amplitude level for a certain wetness content. This allows a calibration curve to be generated from the sensor response, which helps to determine an unknown wetness content in a corresponding leaf type. Such calibration curves typically have a plant-specific characteristic and therefore, it can be inferred that the designed leaf wetness detector provides an optimum solution for plant health monitoring in any small-scale gardening applications. The depicted analysis in this paper provides a laboratory-based proof of concept of the sensing system. A pilot study on the real-world deployment of the system using chipless readers is currently being carried out by the authors. Based on the obtained sensing data and leaf morphology information from this study, the authors plan to perform a machine learning algorithm-based analysis. This will enable the determination of more precise calibration curves for all the leaf samples being used in the pilot project. The proposed sensor has a very good commercialization potential which can certainly be furthered by undertaking a multidisciplinary research approach. For example, increasing the conductivity of the conductive ink will aid the improvement of resonator quality factor which will eventually augment the overall sensing capability and resolution of the proposed sensor.

REFERENCES

[1] D. Evans. (2012). *The Internet of Everything*. Accessed: Jan. 18, 2018. [Online]. Available: https://www.cisco.com/c/dam/global/en_my/assets/ciscoinnovate/pdfs/IoE.pdf

[2] A. Krigman. Globalsign.com. (2018). *From Connected Cows and Crop Control to Drones, The Internet of Things is Rapidly Improving Agriculture*. Accessed: Feb. 4, 2019. [Online]. Available: https://www.globalsign.com/en/blog/connected-cows-and-crop-control-to-drones-the-internet-of-things-is-rapidlyimproving-agriculture/

[3] D. M. Dobkin, *The RF in RFID: Passive UHF RFID in Practice*. Amsterdam, The Netherlands: Elsevier, 2007.

[4] M. A. Islam and N. C. Karmakar, "A novel compact printable dual-polarized chipless RFID system," *IEEE Trans. Microw. Theory Techn.*, vol. 60, no. 7, pp. 2142–2151, Jul. 2012.

[5] S. Dey and N. C. Karmakar, "Chipless RFID strain sensors: A novel feasibility analysis in terms of conventional patch antennas," in *Proc. IEEE MTT-S Int. Microw. RF Conf. (IMaRC)*, Dec. 2015, pp. 72–75.

[6] P. Harrop and R. Das. (2011). *Printed and Chipless RFID Forecasts, Technologies & Players 2009—2029*. Accessed: Jun. 14, 2015. [Online]. Available: http://media2.idtechex.com/pdfs/en/R9034K8915.pdf

[7] T. Rowlandson, M. Gleason, P. Sentelhas, T. Gillespie, C. Thomas, and B. Hornbuckle, "Reconsidering leaf wetness duration determination for plant disease management," *Plant Disease*, vol. 99, no. 3, pp. 310–319, 2015.

[8] S. Dadshani, A. Kurakin, S. Amanov, B. Hein, H. Rongen, S. Cranstone, U. Blievernicht, E. Menzel, J. Léon, N. Klein, and A. Ballvora, "Non-invasive assessment of leaf water status using a dual-mode microwave resonator," *Plant Methods*, vol. 11, no. 1, pp. 1–10, Dec. 2015.

[9] W. D. Jones. New Device Lets Plants Talk. IEEE Spectrum: Technology, Engineering, and Science News, 2009. Accessed: Feb. 5, 2017. [Online]. Available: http://spectrum.ieee.org/consumer-electronics/gadgets/new-device-lets-plants-talk

[10] T. L. Rowlandson, "Leaf wetness: Implications for agriculture and remote sensing," Ph.D. dissertation, Dept. Agronomy, Iowa State Univ., Ames, IA, USA, 2011, doi: 10.31274/etd-180810-3854.

[11] G. Blackwell. Wi-fiplanet.com. (2004). *The Wireless Winery*. Accessed: Feb. 5, 2017. [Online]. Available: http://www.wi-fiplanet.com/columns/article.php/3412061/The-Wireless-Winery.htm

[12] Decagon.com. (2012). *LWS Leaf Wetness Sensor*. Accessed: Feb. 5, 2017. [Online]. Available: https://www.decagon.com/en/canopy/canopy-measurements/lws-leaf-wetness-sensor

[13] Agrihouse.com. (2016). *Leaf Sensor Rev3*. Accessed: Feb. 6, 2017. [Online]. Available: http://www.agrihouse.com/secure/shop/item.aspx?itemid=134

[14] T. Schmugge, "Chapter 5: Remote sensing of soil moisture," in *Hydrological Forecasting*, M. G. Anderson and T. P. Burt, Eds. New York, NY, USA: Wiley, 1985, pp. 101–124.

[15] J. P. Walker, "Estimating soil moisture profile dynamics from near-surface soil moisture measurements and standard meteorological data," Ph.D. dissertation, Dept. Civil, Surveying Environ. Eng., Univ. Newcastle, Callaghan, NSW, Australia, 1999. [Online]. Available: http://users.monash.edu.au/~jpwalker/talks/PhD-Sem/

[16] D. C. Elton, "Understanding the dielectric properties of water," Ph.D. dissertation, Dept. Phys. Astron., Stony Brook Univ., Stony Brook, NY, USA, 2016. [Online]. Available: https://ui.adsabs.harvard.edu/abs/2016PhDT....50E

[17] A. R. von Hippel, Ed., *Dielectric Materials and Applications*. Cambridge, MA, USA: MIT Press, 1954.

[18] V. I. Minkin, O. A. Osipov, Y. A. Zhdanov, and W. E. Vaughan, "Basic principles of the theory of dielectrics," in *Dipole Moments in Organic Chemistry*, W. E. Vaughan Ed. Boston, MA, USA: Springer, 1970, pp. 1–40.

[19] J. A. Lane and J. A. Saxton, "Dielectric dispersion in pure polar liquids at very high radio frequencies. III. The effect of electrolytes in solution," *Proc. Roy. Soc. London. Ser. A, Math. Phys. Sci.*, vol. 214, no. 1119, pp. 531–545, 1952. [Online]. Available: www.jstor.org/stable/99016

[20] M. Dobson, F. Ulaby, M. Hallikainen, and M. El-Rayes, "Microwave dielectric behavior of wet soil—Part II: Dielectric mixing models," *IEEE Trans. Geosci. Remote Sens.*, vol. GE-23, no. 1, pp. 35–46, Jan. 1985, doi: 10.1109/TGRS.1985.289498.

[21] A. Kapoor, P. K. Varshney, and M. J. Akhtar, "Interdigital capacitor loaded electric-LC resonator for dielectric characterization," *Microw. Opt. Technol. Lett.*, vol. 62, no. 9, pp. 2835–2840, Sep. 2020, doi: 10.1002/mop.32391.

[22] P. K. Varshney, A. Sharma, and M. J. Akhtar, "Exploration of adulteration in some food materials using high-sensitivity configuration of electric-LC resonator sensor," *Int. J. RF Microw. Comput.-Aided Eng.*, vol. 30, no. 2, p. 22045, Feb. 2020, doi: 10.1002/mmce.22045.

[23] W. Withayachumnankul, C. Fumeaux, and D. Abbott, "Compact electric-LC resonators for metamaterials," *Opt. Express*, vol. 18, no. 25, pp. 25912–25921, Nov. 2010.

[24] T. Markovic, J. Bao, G. Maenhout, I. Ocket, and B. Nauwelaers, "An interdigital capacitor for microwave heating at 25 GHz and wideband dielectric sensing of nL volumes in continuous microfluidics," *Sensors*, vol. 19, no. 3, p. 715, Feb. 2019, doi: 10.3390/s19030715.

[25] J. Yeo and J.-I. Lee, "High-sensitivity microwave sensor based on an interdigital-capacitor-shaped defected ground structure for permittivity characterization," *Sensors*, vol. 19, no. 3, p. 498, Jan. 2019, doi: 10.3390/s19030498.

[26] Satoaustralia.com. *SATO Australia | CLNX Series*. Accessed: Apr. 8, 2018. [Online]. Available: https://www.satoaustralia.com/products/printers/industrial-printers/clnx-series.aspx

[27] F. Babaeian and N. C. Karmakar, "Hybrid chipless RFID tags—A pathway to EPC global standard," *IEEE Access*, vol. 6, pp. 67415–67426, 2018, doi: 10.1109/ACCESS.2018.2879050.

[28] F. Babaeian and N. C. Karmakar, "A high gain dual polarized ultra-wideband array of antenna for chipless RFID applications," *IEEE Access*, vol. 6, pp. 73702–73712, 2018, doi: 10.1109/ACCESS.2018.2883439.

[29] K. Blattenberger. Rfcafe.com. *Dielectric Constant, Strength, & Loss Tangent—RF Cafe*. Accessed: Sep. 7, 2017. [Online]. Available: http://www.rfcafe.com/references/electrical/dielectric-constants-strengths.htm

[30] M. M. Forouzandeh and N. Karmakar, "Towards the improvement of frequency-domain chipless RFID readers," in *Proc. IEEE Wireless Power Transf. Conf. (WPTC)*, Jun. 2018, pp. 1–4.

[31] J. Aliasgari, M. Forouzandeh, and N. Karmakar, "Chipless RFID readers for frequency-coded tags: Time-domain or frequency-domain?" *IEEE J. Radio Freq. Identificat.*, vol. 4, no. 2, pp. 146–158, Jun. 2020, doi: 10.1109/JRFID.2020.2982822.

[32] Sparkfun.com. *Walabot Developer-SEN-14535—SparkFun Electronics*. Accessed: May 26, 2020. [Online]. Available: https://www.sparkfun.com/products/14535

SHUVASHIS DEY (Member, IEEE) received the B.Tech. degree in electronics and communication engineering from the National Institute of Technology-Durgapur, India, in 2007, the M.Sc. degree in wireless networks from Queen Mary, University of London, U.K., in 2009, and the Ph.D. degree in electrical and computer systems engineering (ECSE) from Monash University, Australia, in 2018.

He is currently a Postdoctoral Research Fellow with the Department of ECSE, Monash University, Australia. Since 2016, he has been a Research Affiliate with the Auto-ID Labs, Massachusetts Institute of Technology (MIT), Cambridge, USA. From 2010 to 2013, he was a Lecturer with the American International University-Bangladesh (AIUB), Dhaka, Bangladesh. His research interests include the microwave devices and antennas, wearable antennas for healthcare applications, chipless and chip-based UHF RFID tag and sensors, and the Internet of Things (IoT).

Dr. Dey received several awards and honors, including the Young Scientist's Travel Grant at the 2012 IEEE International Symposium on Antennas and Propagation (ISAP), the IEEE MTT-S Ph.D. Student Sponsorship Initiative Award in 2016, and the Best Presentation Award at International Conference on Sensing Technology (ICST) in 2017.

EMRAN MD. AMIN (Member, IEEE) received the Ph.D. degree from the Electrical and Computer Systems Engineering Department, Monash University, Australia.

He was a Visiting Research Scholar at the Massachusetts Institute of Technology (MIT), USA. He is currently working with Radio Frequency Systems (RFS), as an Research and Development Design Engineer and a Project Team Leader. He has a successful multi-disciplinary research career for the last seven years in the areas of electrical and electronic systems, pervasive sensors, radio frequency identification (RFID) sensor system, wireless communications, digital signal processing, power electronics, smart sensing materials, and microwave sensors for biomedical applications. His research vision is to deliver a technology that would replace optical barcodes with passive, sub-cent, highly sensitive, and fully printable chipless RFID sensors. Such low-cost ubiquitous sensing technology can uniquely identify and monitor each and every physical object through Internet of Things (IoT). He is also working with a number of pioneer research groups, namely the AutoID Lab, Massachusetts Institute of Technology (MIT), the Monash Microwave Antennas RFID and Sensors (MMARS) Lab, and the Monash Conducting Polymer research group.

Dr. Amin is a frequent Reviewer for prestigious journals and conference papers, including IEEE TRANSACTIONS ON MICROWAVE THEORY AND TECHNIQUES (MTT) and IEEE SENSORS JOURNAL.

NEMAI CHANDRA KARMAKAR (Senior Member, IEEE) received the B.Sc. degree in electrical and electronic engineering from the Bangladesh University of Engineering and Technology, the M.Sc. degree in electrical engineering from the University of Saskatchewan, Canada, and the Ph.D. degree in information technology and electrical engineering from The University of Queensland, St. Lucia, QLD, Australia, in 1999.

He is an Associate Professor with the Department of Electrical and Computer Systems Engineering, Monash University, Clayton, VIC, Australia. He has 20 years of teaching, design, and research experience in smart antennas, microwave active and passive circuits, and chipless RFIDs in both industry and academia in Australia, Canada, Singapore, and Bangladesh. He has authored or coauthored more than 230 refereed journal and conference papers, 24 refereed book chapters, and three edited and one coauthored book in RFID. He has two patent applications for chipless RFIDs. His research interests include chipless RFID and RF sensors, microwave antenna, signal processing, digital design, fabrication, integration, smart antenna for mobile and satellite communication, electromagnetic band gap structure (EBG) assisted RF devices, planar phased array antennas, beamforming networks, and microwave device modeling.